Check for updates

Received: 24 November 2021 | Revised: 16 June 2022 | Accepted: 22 June 2022

DOI: 10.1002/jcb.30303

RESEARCH ARTICLE

Journal of Cellular Biochemistry WILEY

The activation of M2 muscarinic receptor inhibits cell growth and survival in human epithelial ovarian carcinoma

Marilena Taggi[1] | **Andjela Kovacevic**[1] | **Chiara Capponi**[1] | **Marta Falcinelli**[1] | **Veronica Cacciamani**[1] | **Elena Vicini**[1] | **Rita Canipari**[1] | **Ada Maria Tata**[2]

[1]Department of Anatomy, Histology, Forensic Medicine and Orthopedic, Section of Histology, Sapienza University of Rome, Rome, Italy

[2]Department of Biology and Biotechnologies Charles Darwin, Sapienza University of Rome, Rome, Italy

Correspondence
Elena Vicini and Rita Canipari, Department of Anatomy, Histology, Forensic Medicine and Orthopedic, Section of Histology, Sapienza University of Rome, Rome, Italy.
Email: elena.vicini@uniroma1.it and Rita.canipari@uniroma1.it

Present address
Marta Falcinelli, School of Pharmacy and Biomolecular Sciences, Centre for Stress and Age-related Disease, University of Brighton, Moulsecoomb, BrightonBN2 4GJ, UK.

Funding information
Ateneo Sapienza; Ministry of Research MIUR Grant PRIN 2017, Grant/Award Number: 2017TK7Z8L

Abstract

Ovarian cancer is the fifth leading cause of cancer-related deaths in females. Many ovarian tumor cell lines express muscarinic receptors (mAChRs), and their expression is correlated with reduced survival of patients. We have characterized the expression of mAChRs in two human ovarian carcinoma cell lines (SKOV-3, TOV-21G) and two immortalized ovarian surface epithelium cell lines (iOSE-120, iOSE-398). Among the five subtypes of mAChRs (M1–M5 receptors), we focused our attention on the M2 receptor, which is involved in the inhibition of tumor cell proliferation. Western blot analysis and real-time PCR analyses indicated that the levels of M2 are statistically downregulated in cancer cells. Therefore, we investigated the effect of arecaidine propargyl ester hydrobromide (APE), a preferential M2 agonist, on cell growth and survival. APE treatment decreased cell number in a dose and time-dependent manner by decreasing cell proliferation and increasing cell death. FACS and immunocytochemistry analysis have also demonstrated the ability of APE to accumulate the cells in G2/M phase of the cell cycle and to increase the percentage of abnormal mitosis. The higher level of M2 receptors in the iOSE cells rendered these cells more sensitive to APE treatment than cancer cells. The data here reported suggest that M2 has a negative role in cell growth/survival of ovarian cell lines, and its downregulation may favor tumor progression.

KEYWORDS
apoptosis, mitotic catastrophe, muscarinic receptors, ovarian cancer, ovarian epithelial cells

This is an open access article under the terms of the Creative Commons Attribution-NonCommercial-NoDerivs License, which permits use and distribution in any medium, provided the original work is properly cited, the use is non-commercial and no modifications or adaptations are made.
© 2022 The Authors. *Journal of Cellular Biochemistry* published by Wiley Periodicals LLC.

1 | INTRODUCTION

Ovarian cancer is the fifth leading cause of cancer-related deaths in females. Greater than 95% of ovarian cancers originate in the epithelial cells on the ovary surface (OSE), a derivative of the embryonic coelomic epithelium that takes part in the cyclical ovulatory ruptures and repair.

The mechanisms of epithelial ovarian cancer development have been long debated, and different hypotheses have been proposed. The "Gonadotropin hypothesis" proposes that the hormonal environment of the OSE, as high gonadotropin levels, can have a role in promoting neoplastic transformation by regulating the proliferative activity of OSE cells.[1,2] The high gonadotropin levels found in cysts and peritoneal fluid from ovarian cancer patients support this hypothesis.[3] The second one is the "incessant ovulation hypothesis," first proposed in 1971,[4] according to which repeated episodes of ovulation-associated injury and repair of the OSE cells could induce mutations in these cells and later malignancies.

The ovulatory process itself resembles an inflammatory reaction, with leukocytic infiltration, release of inflammatory cytokines, vasodilatation, DNA repair, and tissue remodeling. Several inflammatory factors, such as cytokines secreted by the infiltrating leukocytes, have been implicated in ovarian carcinogenesis. Epidemiological evidence suggests that ovarian cancer may be related to chronic inflammatory processes (e.g., endometriosis, pelvic inflammatory disease, or mumps viral infection). The alteration in the expression of genes associated with inflammation[5] and the reduction of local inflammation (e.g., tubal ligation and hysterectomy) appear to reduce the risk of ovarian cancer. Moreover, the lower incidence of ovarian cancer has been associated with women taking anti-inflammatory medications.[6]

Various studies have reported that the cholinergic system, with its components acetylcholine (ACh), nicotinic and muscarinic receptors (mAChRs), is expressed not only in the brain but can be found in many different organ systems such as cardiovascular, respiratory, digestive systems, and reproductive tracts. ACh's action is mediated by mAChRs, G-protein coupled receptors expressed in neuronal and nonneuronal tissues.[7,8] Five muscarinic subtypes have been cloned in different animal species (M1–M5). These receptors present a high homology degree but significant variability in the carboxy- and amino-terminals and the third cytoplasmic loop. They are involved in controlling cell proliferation by activating pathways such as IP3K and MAPK/ERK kinases.

Numerous groups have described that ACh, via mAChRs, can modulate migration, proliferation, and angiogenesis in several tumor types such as colon, ovarian, lung, breast cancer,[9] melanoma,[10] neuroblastoma[11] and glioblastoma,[12–15] and inflammatory processes in the lung.[16]

In the ovary, studies by Mayerhofer and co-workers[7,8] have demonstrated the presence of the cholinergic autocrine system. Granulosa cells of antral follicles in the rhesus monkey and human ovary contain choline acetyltransferase and produce ACh under follicle stimulating hormone (FSH) stimulation, suggesting cholinergic autocrine/paracrine signals regulating the ovarian function. Moreover, granulosa cells express M1 and M5 receptor subtypes, while the oocytes express the M3 subtype.[17]

In the ovarian tumors, a correlation was observed[18] between positive mAChR status of ovarian tumor cell lines and reduced survival time of the patients from whom the tumor cells were derived. Initial studies[19] showed mAChRs in ovarian tumors and tumor cell lines, and the binding profile suggested the presence of M3 receptor subtype. Altogether, these results suggest a significant correlation between high levels of mAChRs and an adverse prognosis of patients with ovarian carcinoma.

Although these studies highlight the influence of mAChRs in ovarian cancer progression, the mAChR subtypes' expression in ovarian cancer cells has been poorly investigated.

The present study aimed to investigate better the mAChR subtypes' expression in ovarian cancer cells and nontumoral iOSE cells. We focused our attention on the M2 receptor, a receptor involved in inhibiting tumor cell proliferation in other cancer cell lines and whose function has never been studied in ovarian cancer.

2 | EXPERIMENTAL PROCEDURES

2.1 | Cell culture

Human ovarian carcinoma cell lines (TOV-21G, SKOV-3) were purchased from ATCC; iOSE cells (iOSE-120, iOSE-398) were kindly provided by Dr. David Huntsman, Canadian OvCaRe Cell Bank, British Columbia Cancer Research Centre, Vancouver, B.C. Canada. TOV-21G cells were cultured in a 1:1 mixture of MCDB 131 medium and Medium 199 supplemented with 15% fetal bovine serum (FBS); SKOV-3 in RPMI-1640 medium supplemented with 10% FBS and iOSE in a 1:1 mixture of MCDB 105 medium and Medium 199 supplemented with 5% FBS. All media were supplemented with 1% streptomycin/penicillin, 1% glutamine. Sigma-Aldrich supplied all reagents for cell cultures.

2.2 | Muscarinic agonist and antagonist treatments

M2 mAChR agonist, arecaidine propargyl ester hydrobromide (APE; Sigma-Aldrich), was used at different concentrations (from 25 to 100 μM). The APE selectivity for M2 receptor was confirmed by pharmacological binding experiments using different mAChR antagonists.[15,20] mAChR antagonists were used at the final concentration of 10^{-6} M for Gallamine (M2 antagonist; CliniSciences), 10^{-7} M for Pirenzepine (M1 antagonist; Sigma-Aldrich), and 10^{-8} M for 4-DAMP (M3–M5 antagonist; Sigma-Aldrich).[15] The cells were pre-incubated for 2 h with the antagonists before APE treatment. Cell lines were also treated with Muscarine chloride hydrate (Sigma-Aldrich) an agonist of all mAChRs, at the final concentration of 100 μM, according to previous studies.[21]

2.3 | Cell growth

To analyze cell growth, we plated the cells in 12-well plates at a density of 3×10^4 cells/well. Twenty-four hours after plating, the cells were treated with increasing APE concentrations for 1–3 days. At the end of the treatments, adherent and floating cells were combined and stained with Trypan Blue. Viable cells were evaluated using a hemocytometer.

2.4 | Evaluation of cell death by propidium iodide (PI) staining

The cells were plated in 35-mm dishes at a density of 7×10^4 cells/dish. The following day, cells were treated with APE (50 and 100 μM) for 48 h. At the end of the treatment, cells were trypsinized and resuspended in phosphate-buffered saline (PBS)/FBS 1:1. Then the samples were incubated with 2 μg/ml PI (Sigma-Aldrich) for 30min at room temperature (RT) and subjected to FACS analysis using CyAn ADP flow cytometer. Samples were analyzed with FlowJo software, version 10.5.3.

2.5 | Annexin V staining for apoptosis detection

Annexin V analysis for apoptosis detection was performed using eBioscience™ Annexin V-APC Apoptosis Detection Kit (Thermo Fisher Scientific) according to the manufacturer's instructions. Cells were treated with APE 100 μM at different times (4–8–24 h) at the density of 1.5×10^5 cells/dish. At the end of the treatment, cells were trypsinized, washed twice with PBS1X, and incubated with staining solution for 15 min at RT in the dark. Samples were run on the BD FACSCanto II and analyzed with BD FACSDiva Software (BD Biosciences).

2.6 | Total RNA preparation, reverse transcription polymerase chain reaction (RT-PCR), and real-time PCR

Total RNA was extracted using TRI-Reagent (Sigma-Aldrich). Total RNA was reverse-transcribed in a final volume of 20 μl using the M-MLV Reverse Transcriptase kit (Invitrogen) according to the manufacturer's instructions. The expression of human mAChR subtypes was evaluated by semiquantitative RT-PCR using One-Step RT-PCR Kit (GeneDireX). RPLP0 was used as the housekeeping gene. The presence of transcripts for mAChRs and apoptotic markers was also evaluated by SYBR Green Real-Time PCR on an Applied Biosystems Real-Time PCR System using SYBR Green Universal PCR Master Mix (EuroClone), following the manufacturer's recommendations. Each sample was normalized to its RPS29 or RPLP0 content. The primers utilized are described in the Supporting Information: Table S1. Primer's specificity was confirmed by melting curves.

2.7 | Western blot analysis

After treatments, the cells were lysed in 150 μl of lysis buffer 1X (CST) containing 1 mM phenylmethylsulfonyl fluoride (Sigma-Aldrich). Protein concentration was measured by BCA protein assay kit (Pierce Biotechnology). Samples containing equal amounts of proteins (50 μg) were subjected to SDS-PAGE on a 10% or 15% acrylamide gel[22] and transferred onto a nitrocellulose membrane (Schleicher & Schuell, Whatman GmbH). The filters were blocked for 2 h in Tris-buffered saline-Tween 20 (TBST) and then incubated overnight at 4°C with the primary antibodies. The mouse anti-Muscarinic Acetylcholine Receptor M2/CHRM2 monoclonal IgG1 (1:800, NB120-2805; Novus Bio), rabbit anticleaved caspase 3 (1:500, #9661; CST) were used. Glyceraldehyde-3-phosphate dehydrogenase (1:500, sc-47724; Santa Cruz Biotechnology) and tubulin (1:500, T5168; Sigma-Aldrich) were used to normalize the intensity of the bands. Membranes were incubated with secondary HRP antibodies (anti-mouse, sc-2005, anti-rabbit, sc-2305, 1:10000; Santa Cruz Biotechnology) for 1 h at RT. Signals were detected by an ECL immunodetection system (Amersham

Corp.) following the manufacturer's instruction and visualized by Chemi DocTM XRS 2015 (Bio-Rad Laboratories). Densitometric analysis of the bands was performed using Image Lab software (version 5.2.1; Bio-Rad Laboratories).

2.8 | Immunocytochemistry analysis

Cells at subconfluence were fixed with 4% paraformaldehyde (PFA)/PBS for 10 min at 4°C, washed twice with PBS 1X, and incubated with 3% BSA (Sigma-Aldrich) and 0.5% TritonX-100 for 10 min at RT. The reduction of nonspecific background signal was obtained by incubating cells with 1 M glycine (Sigma-Aldrich) and subsequently with block solution consisting of 0.5% Triton X-100, 3% BSA, and 5% normal donkey serum (Jackson Laboratories Immuno Research) for 30min at RT. The cells were incubated with the following primary antibodies: mouse anti-α tubulin (T5168; 1:500; Sigma-Aldrich) and rat anti-PHH3 (phosphorylated histone H3) (1:100; Abcam, ab10543) for 1 h at RT. After the washes, the cells were incubated with species-specific secondary antibodies Alexa Fluor® 488 AffiniPure Donkey Anti-Mouse IgG (H+L) and Cy3-AffiniPure Donkey Anti-Rat IgG (H+L) (#715-545-150 and #712-165-153, respectively; Jackson Immuno Research), diluted 1:200 for 1 h at RT. Nuclei were then counterstained with TO-PRO-3 Iodide (642/661) (T3605; Life Technologies), and the slides were closed with Vectashield mounting medium (Vector Laboratories). Pictures were acquired using a Leica TCS SP2 confocal microscope.

2.9 | 5-Bromo-2′-deoxyuridine (BrdU) cell proliferation assay

The cells at the exponential phase were treated with increasing APE concentrations for 48 h. At the end of treatment, BrdU (Sigma-Aldrich) was added to the medium at a final concentration of 45μM for 20 min. Samples were fixed with 4% PFA/PBS for 10min at 4°C. Partial DNA denaturation was performed using 3.5 N HCl for 3 min at RT. The cells were permeabilized in 0.1% TritonX-100 for 10 min at RT; the reduction of nonspecific background signal was obtained as described for immunofluorescence. Samples were then incubated with rat anti-BrdU (1:50; Abcam, ab6326) for 1 h at RT. After the washes, the cells were incubated with species-specific secondary antibody for 1 h at RT (Donkey Anti-Rat IgG (H+L)-FITC; Jackson Immuno Research, #712-545-153, diluted 1:200). In the end, the nuclei were stained with 1 μg/ml Hoechst-33342. After two washes for 5 min each in PBS, the slides were mounted with buffered glycerol and examined using a Zeiss Axioscope Imager 2 fluorescence microscope (Carl Zeiss SpA). Pictures were acquired at a magnification of 10×. Total (an average of 3000 cells) and BrdU positive cells were counted in 20 randomly chosen fields, and the percentages of total BrdU positive cells out of the totals were quantified.

2.10 | Nuclear staining

For nuclear morphological analysis, both floating and adherent cells were fixed in 4% PFA/PBS. Floating cells were cytocentrifuged onto a glass slide at 1000 rpm for 20 min. After fixation the cells were washed with PBS and then incubated for 12 min with 1 μg/ml Hoechst-33342. Staining was visualized on a Zeiss Axioscope Imager 2 fluorescence microscope (Carl Zeiss SpA).

2.11 | Statistical analysis

Statistical analyses were performed using one-way analysis of Variance followed by the Student–Newman–Keuls method to compare multiple groups. Values with $p < 0.05$ were considered statistically significant.

3 | RESULTS

3.1 | Characterization of mAChRs in ovarian tumor cell lines and nontumor immortalized cell lines

RT-PCR and real-time PCR determined mAChR transcripts in two ovarian cancer cell lines, SKOV-3 and TOV-21G, and two immortalized nontumorigenic human OSE cell lines iOSE398 and iOSE120. Except for M4 (not shown), all the other receptors were found in the four cell lines (Figure 1A). We focused our attention on M2 receptor. The real-time PCR analysis confirmed that M2 mRNA levels were significantly higher in the two iOSE cells than cancer cell lines (Figure 1B). When reverse transcriptase was omitted, no bands were detectable, indicating the absence of genomic DNA contamination (data not shown). The higher levels of M2 in OSE cells were also confirmed at the protein level by western blot analysis (Figure 1C).

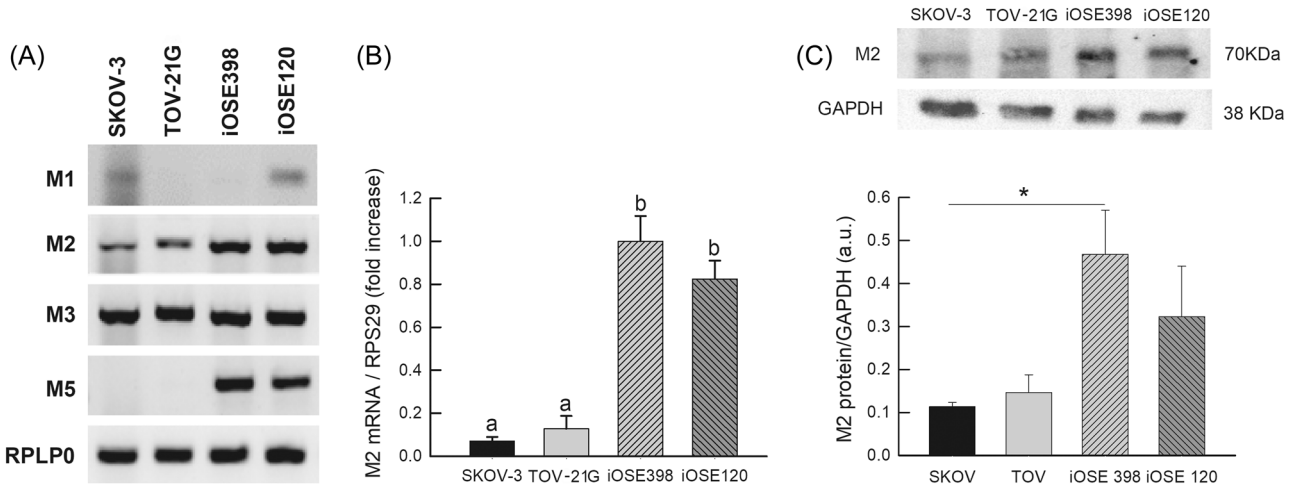

FIGURE 1 Characterization of mAChRs in ovarian cancer cells and immortalized ovarian surface epithelium cell lines. (A) Representative RT-PCR analysis of muscarinic receptor transcript expression in two cancer cell lines (SKOV-3 and TOV-21G) and two immortalized nontumorigenic human OSE cell lines (iOSE-120, iOSE-398) of three independent cell cultures. (B) Levels of expression of M2 muscarinic receptor transcripts by Real Time-PCR in the different cell lines. Values are expressed as fold increase respect to iOSE398 values, arbitrarily set to 1. Values with the different superscript letters indicate statistical significance ($p < 0.05$) between groups. (C) Representative western blot analysis of M2 protein expression in ovarian cancer cells and immortalized ovarian surface epithelium cell lines. Densitometric absorbance values from three independent experiments were averaged (±SEM) and are expressed as arbitrary units (a.u.). GAPDH was used as internal control. *$p < 0.05$. GAPDH, glyceraldehyde-3-phosphate dehydrogenase; mAChR, muscarinic receptor.

3.2 | M2 receptor is involved in the inhibition of ovarian cancer cell proliferation

To investigate the possible role of M2 receptor in the control of cell growth and survival, we treated the cells with a selective M2 agonist, APE, at different concentrations, ranging from 25 to 100 μM, and at different culture times. We observed a significant decrease in cell number in response to APE treatment, and the effect was dose and time-dependent in all cell lines (Figure 2A). Moreover, as evidenced by IC50 values (Figure 2A), iOSE cells were more sensitive to the drug than cancer cells.

To confirm that APE effect was mediated by M2 receptor activation, we performed pharmacological competition experiments. The co-treatment for 48 h with APE (50–100 μM) and the M2 antagonist Gallamine, demonstrated the ability of Gallamine to counteract the APE effect on all cell lines (Figure 2B). To exclude a possible contribution of M1, M3, and M5 receptor subtypes in the cell growth inhibition-APE mediated, we used Pirenzepine and 4-DAMP, respectively M1 and M3/M5 antagonists. As shown in Figure 2B, treatment with these antagonists could not counteract APE effects on cell survival, suggesting that the odd mAChRs are not involved. As control of mAChR antagonists' efficiency, we analyzed cell growth in the presence of Muscarine (100 μM), a nonselective mAChR agonist. Muscarine treatment significantly improved cell growth in all cell lines with respect to control conditions (Figure 2C). When we blocked the inhibitory receptor M2 with Gallamine, the addition of Muscarine induced a further improvement in cell proliferation. However, this increase was statistically significant only in the iOSE-120. Conversely, in the presence of the odd mAChR antagonists, we found, as expected, that Muscarine, through M2 receptor, caused a substantial decrease of cell number in all cell lines (Figure 2C).

3.3 | M2 receptor activation affects cell cycle progression

To investigate whether the M2-dependent decrease in cell number could be ascribed to decreased cell proliferation, the fraction of cells in the S-phase was evaluated by bromodeoxyuridine (BrdU) incorporation. In both cancer cell lines and iOSE-120 cells, we observed a decrease in the percentage of cells in the S-phase following APE treatment, which was dose-dependent (Figure 3A–C).

We performed PHH3 counts on both cancer cell lines since PHH3 is a marker of cells within the cell cycle's mitotic phase.[23] PHH3 counts showed that in TOV-21G cell line APE treatment induced a slight

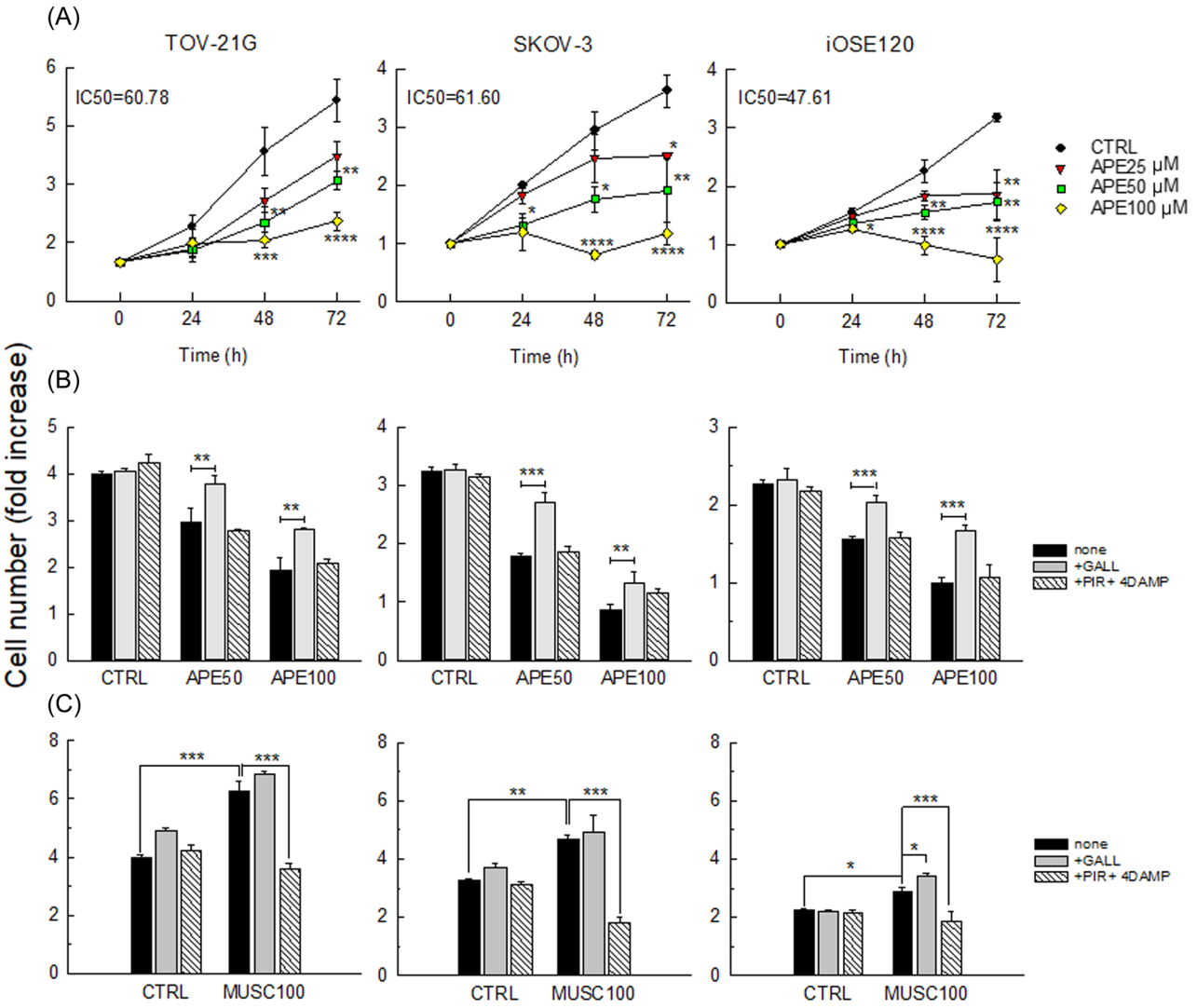

FIGURE 2 APE inhibits cell growth in ovarian cancer cells and immortalized OSE cells. (A) Dose-dependent effect of APE at different times of treatment on cell survival measured by trypan blue staining. Data are the mean ± SEM of three independent experiments performed in triplicate and are expressed as fold increase respect to the number of cells present at time 0 arbitrarily set to 1. *$p < 0.05$; **$p < 0.01$; ***$p < 0.005$; ****$p < 0.001$ versus respective CTRL. Effects of muscarinic receptor antagonists on ovarian cell growth. (B) Cell count performed in ovarian cancer cells and iOSE-120 after 48 h of co-treatment with APE and M2 receptor antagonist Gallamine (1 μM) or APE + Pirenzepine (10^{-7} M) and 4-DAMP (10^{-8} M), respectively M1 and M3/M5 antagonists. (C) Cell count performed in ovarian cancer cells and iOSE-120 after 48 h of co-treatment with Muscarine (100 μM) and Gallamine (1 μM), or Pirenzepine (10^{-7} M) and 4-DAMP (10^{-8} M). All the results are expressed in fold increase respect to t0 arbitrarily set to 1. *$p < 0.05$; **$p < 0.01$; ***$p < 0.001$ versus respective CTRL. APE, arecaidine propargyl ester; CTRL, control.

decrease in the percentage of PHH3 positive cells (Figure 3D). On the contrary, in SKOV-3 cells, APE caused an increase, dose-dependent, of this percentage (Figure 3E), suggesting the accumulation of SKOV-3 in the M phase.

To further investigate this result, we better analyzed all the cell cycle phases in the two cancer cell lines. The analysis of the cell cycle by FACS confirmed that APE treatment induced in SKOV-3 cells a progressive accumulation in G2/M with the time (Figure 3G), while TOV-21G after a transient slowdown in S-phase slowly recovered their growth rate (Figure 3F).

3.4 | M2 receptor activation reduces cell survival inducing cell death

We analyzed by PI staining the effect of APE treatment on cell death. The data obtained demonstrated increased cell death in all cell lines, even with different sensitivity. iOSE cells were the most sensitive to the treatment

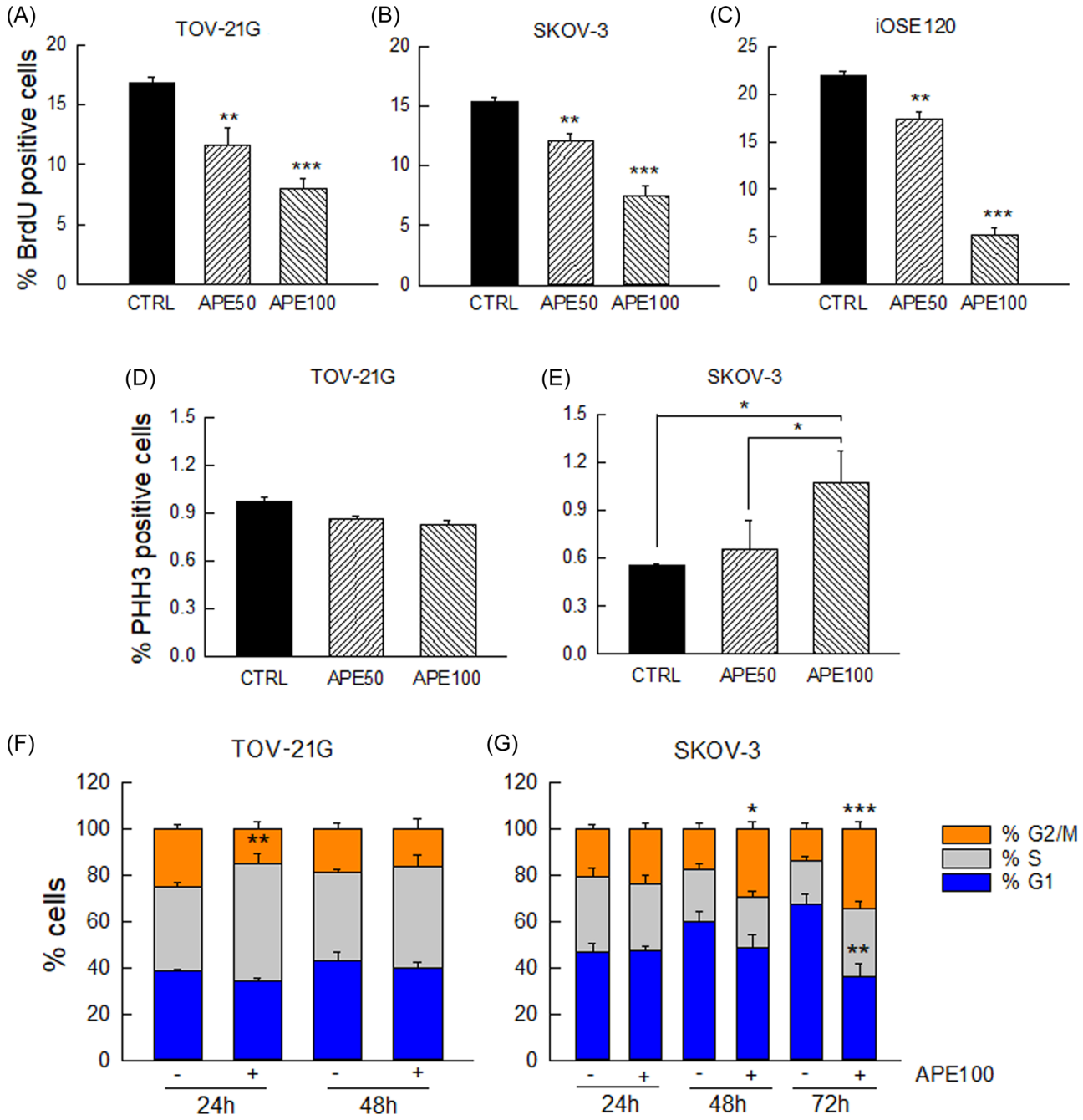

FIGURE 3 APE inhibits cell proliferation in ovarian cancer and iOSE cells (A–C). Data are the mean ± SEM of three independent experiments performed in triplicate and are expressed as percentage of BrdU positive cells. $^{**}p < 0.01$; $^{***}p < 0.001$. An average of 3000 cells was counted in 20 randomly chosen fields for each experiment. (D) and (E) Cells were treated with APE (50 and 100 μM) and then stained with actin and PHH3 antibodies and counterstained with Hoechst-33342. Positive cells were counted, and the data are the mean ± SEM of three independent experiments performed in triplicate and are expressed as percentage of PHH3 positive cells. $^{*}p < 0.05$. An average of 10 000 cells was counted in the whole sample for each experiment. (F) and (G) FACS analysis of cell cycle in TOV-21G and SKOV-3 cell lines. Data are the mean ± SEM of three independent experiments performed in triplicate and are expressed as percentage of cells in G1, S, and G2/M phases. $^{*}p < 0.05$; $^{**}p < 0.005$; $p < 0.001$ versus respective CTRL. APE, arecaidine propargyl ester; CTRL, control.

(Supporting Information: Figure S1), and cancer cells were the most resistant. While the percentage of cell death at 48 h in iOSE was statistically significant at all concentrations tested, in the two cancer cell lines, APE was effective only at the highest concentration (Supporting Information: Figure S1).

Hoechst nuclear staining showed fragmented nuclei (apoptotic nuclei) in TOV-21G, and iOSE-120 APE

treated cells, while SKOV-3 presented nuclei with different morphology, particularly large with uncondensed chromatin (Figure S2a,b).

3.5 | M2 receptor activation induces mitotic catastrophe in SKOV-3 ovarian cancer cells

Considering the accumulation of SKOV-3 cell line in the M phase upon APE treatment, we investigated whether these cancer cells presented abnormal mitosis. We performed an analysis of mitotic spindles of SKOV-3 cell line. Immunofluorescence assays with anti-α-tubulin showed that control cells displayed standard mitotic spindles with chromosomes correctly condensed (Figure 4A). Conversely, treated cells exhibited abnormal mitotic spindles. We observed monopolar or multipolar spindles with significant defects in chromatin condensation (Figure 4B,C). Cells displaying aberrant spindles did not progress through the metaphase–anaphase, and the percentage of aberrant mitosis increased in a dose-dependent manner (Figure 4D). To further confirm these data, we performed the same experiment on TOV-21G cell line (p53 positive cells), and we found only a few aberrant mitoses that did not increase after APE treatment (Figure 4E).

To further investigate the pattern of cell death in the two cancer cell lines, we carried out cytofluorimetric analyses with Annexin V-APC/PI. As shown in Figure 5, with the increase of time, we observed a transient increase of apoptotic cells in TOV-21G cells followed by a secondary increase in necrotic cells. Conversely, in SKOV-3 cells, at the same culture times, we did not observe increasing apoptosis but mainly an increase in necrotic cells.

3.6 | M2 receptor activation can induce different cell death pathways in ovarian cancer cells

Considering the different effects observed in two tumor cell lines, we also investigated the possible apoptotic effects downstream of the M2 agonist treatment. Caspase-3 cleavage is a critical step in apoptosis; therefore, we analyzed the presence of cleaved-caspase3 in response to APE treatment in the different cell lines (Figure 6A–C). In iOSE cell line, we found a dose-dependent increase of activated caspase 3. In TOV-21G, as expected, we observed an increase only at the highest concentrations of APE, while SKOV-3 did not show activation of caspase 3.

To determine which molecular pathway was involved in APE-induced cell death, we investigated by real-time PCR the expression of genes of proapoptotic Bcl2 family (*PUMA*, p53 upregulated modulator of apoptosis, and *NOXA*, Phorbol-12-myristate-13-acetate-induced protein 1) and an antiapoptotic one (*BCL-xL*). *PUMA* expression was induced in TOV-21G and iOSE-120 but not in SKOV-3 (Figure 5D). Conversely, the expression of *NOXA* was induced in all cell lines (Figure 6E). Following APE treatment *BCL-xL* (B-cell lymphoma-extra-large) was slightly downregulated in iOSE-120, in TOV-21G remained unchanged, while in SKOV-3 cells was significantly upregulated (Figure 6F).

4 | DISCUSSION

The cholinergic autocrine loop has been demonstrated in the normal ovary.[7,8] Moreover, it has been reported that ovarian cancer cells express mAChRs.[18] Oppitz et al.[18] described a statistically significant correlation between mAChR status in ovarian carcinoma cell lines and poor prognosis of patients from whom the cell lines were established. However, poor information on the type of receptor present in epithelial ovarian cancer are reported. Initial studies on ovarian adenocarcinoma reported a binding profile whose results suggested the presence of M3 receptors.[19] These receptors are the most common ACh receptors in cancers, and their expression level has been frequently correlated with increased cell proliferation.[24]

The present study aimed to better characterize the expression of the mAChR subtypes in ovarian cancer cells and nontumoral iOSE cells. Our data showed that except for M4, the studied cell lines express all mAChR subtypes, albeit at different levels. Interestingly, the cancer cell lines showed lower levels of M2 receptors. This receptor is involved in the inhibition of tumor cell proliferation in other cancer cell lines[9,11,15,25,26] and its function has never been studied in ovarian cancer.

The control of cell proliferation is a balance of proliferative/antiproliferative effects and may depend on the levels of expression of the different mAChR subtypes. The simultaneous activation of all mAChRs by muscarine, a no selective orthosteric agonist, increased tumor cell number in all treated cell lines. Interestingly, this increase was more evident in cancer cells (Figure 2C), suggesting that the lower levels of M2 in cancer cell lines compared with iOSE, might represent a strategy promoted by the tumor cells to favor cancer cell proliferation.

Moreover, the lower levels of M2 rendered cancer cells less sensitive to M2 agonist APE. In fact, APE

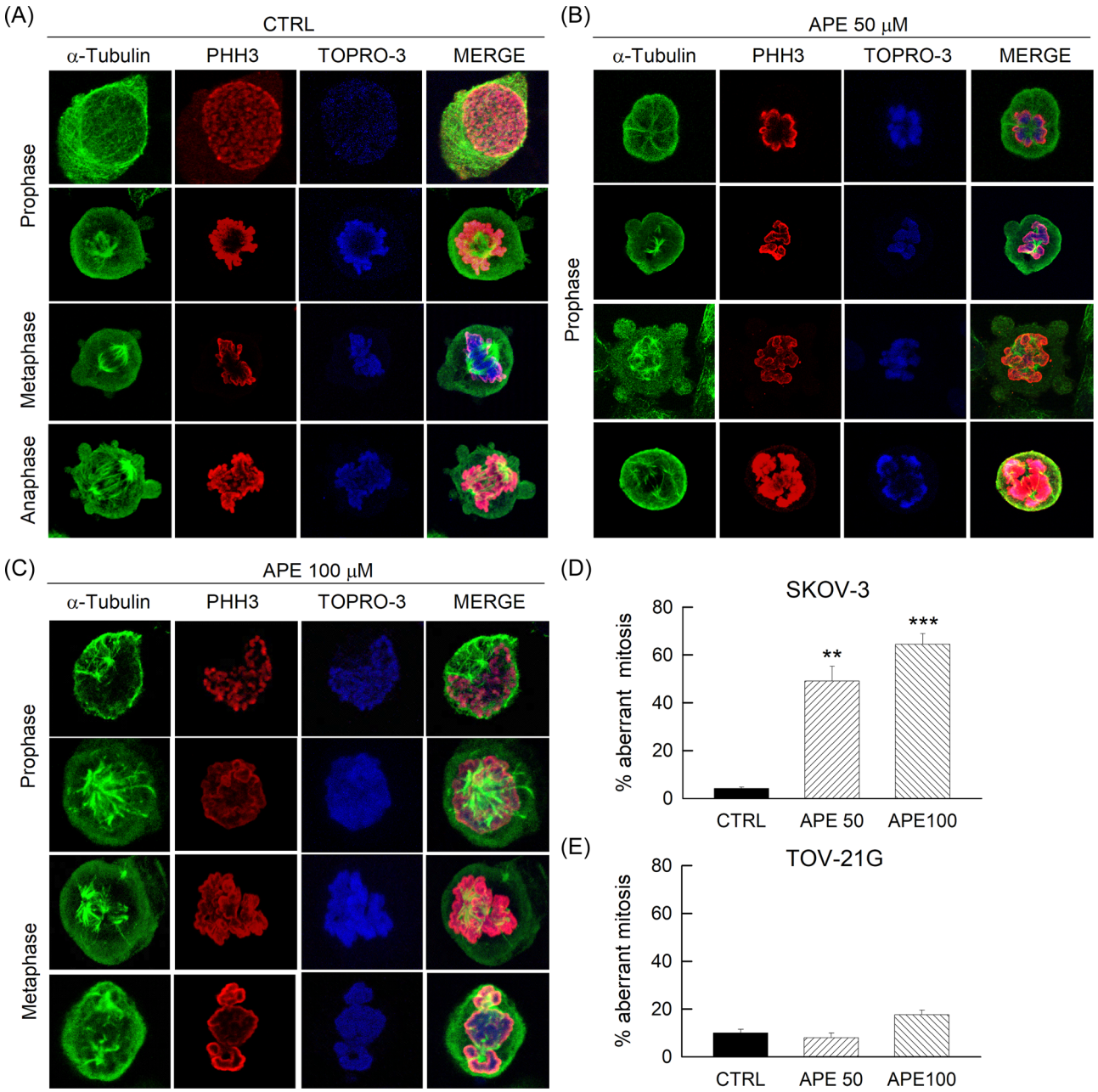

FIGURE 4 APE treatment caused a mitotic catastrophe with abnormal morphology of the mitotic spindle in SKOV-3 cell line. (A)–(C) Mitotic cells have been marked by immunostaining with anti-αtubulin (green), with anti-PHH3 (red) and with TO-PRO3 (blue) in control and treated cells. (D) and (E) Aberrant mitosis counts performed on both cancer cells. Data are the mean ± SEM of three independent experiments performed in triplicate and are expressed as percentage of aberrant mitoses out of 50–60 mitoses observed for each experiment. $^{**}p < 0.01$; $^{***}p < 0.001$ versus CTRL. APE, arecaidine propargyl ester; CTRL, control.

decreased cell growth in all analyzed cell lines in a dose- and time-dependent manner, even though with different sensitivity. The iOSE cells were the most sensitive to the treatment (Figure 2A), and cancer cells were the most resistant.

Interestingly, we found differences in the nuclear morphology after APE treatment. While in the iOSE-120 and the TOV-21G, we observed the presence of fragmented nuclei typically associated with apoptotic processes, in SKOV-3, we found together with cells with fragmented nuclei, the presence of multiple micronuclei and uncondensed chromatin, suggesting that SKOV-3 were dying by mitotic catastrophe as has been recently demonstrated in U251 cells.[27]

To better understand the impact of APE on cell proliferation, we have analyzed, by FACS analysis, the cell cycle progression in the two cancer cell lines. While TOV-21G recovered to the normal cycle after an initial

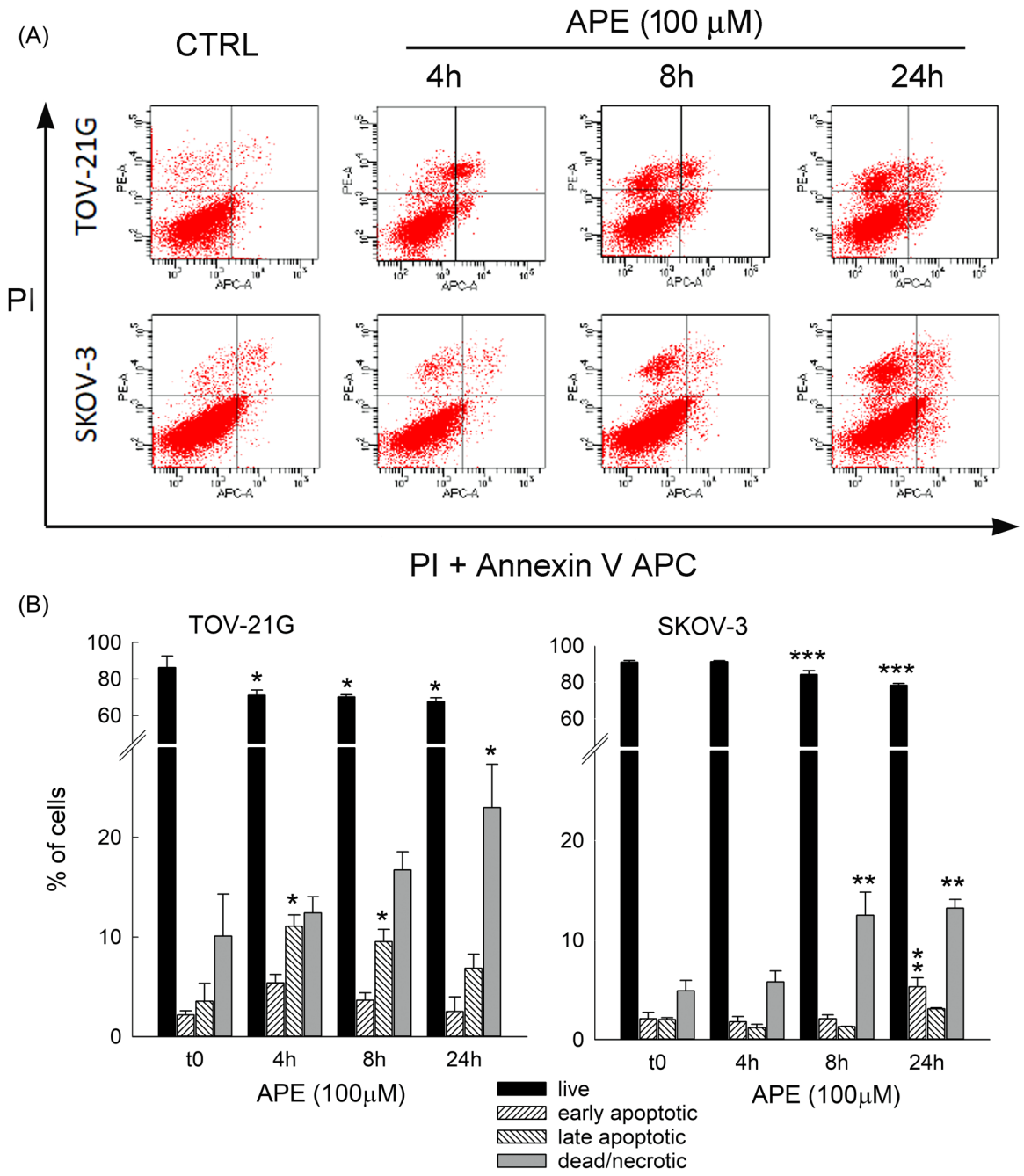

FIGURE 5 APE treatment induced cell death in both cell lines. (A) Representative cytofluorimetric analysis for Annexin V/PI staining of TOV-21G and SKOV-3 cell lines cultured for different times in the presence of 100 μM APE. (B) Graphs represent the mean ± SEM of three independent experiments and are expressed as the percentage of cell population. *$p < 0.05$; **$p < 0.01$; ***$p < 0.001$ versus CTRL. APE, arecaidine propargyl ester; CTRL, control.

transient slowdown in the G1/S phase, SKOV-3 cells slowly accumulated in the G2/M phase. The increase of PHH3 positive cells has demonstrated that only the SKOV-3 accumulated in the cell cycle M phase.

These different responses to M2 activation may also depend on the different status of p53 in our cells; in fact, iOSE-120 and TOV-21G express p53 wild-type that was positively regulated by APE treatment (data not shown), while SKOV-3 cells do not express p53 at the protein or mRNA level.[28] Therefore, the absence of p53 protein may render this cell line unable to recover the cell damage induced by APE treatment.

Upon spindle damage, cells become arrested at the metaphase–anaphase transition point, escape from the block (mitotic slippage), and are definitively arrested at the G1 stage. P53 mediates this arrest[29] and, as previously

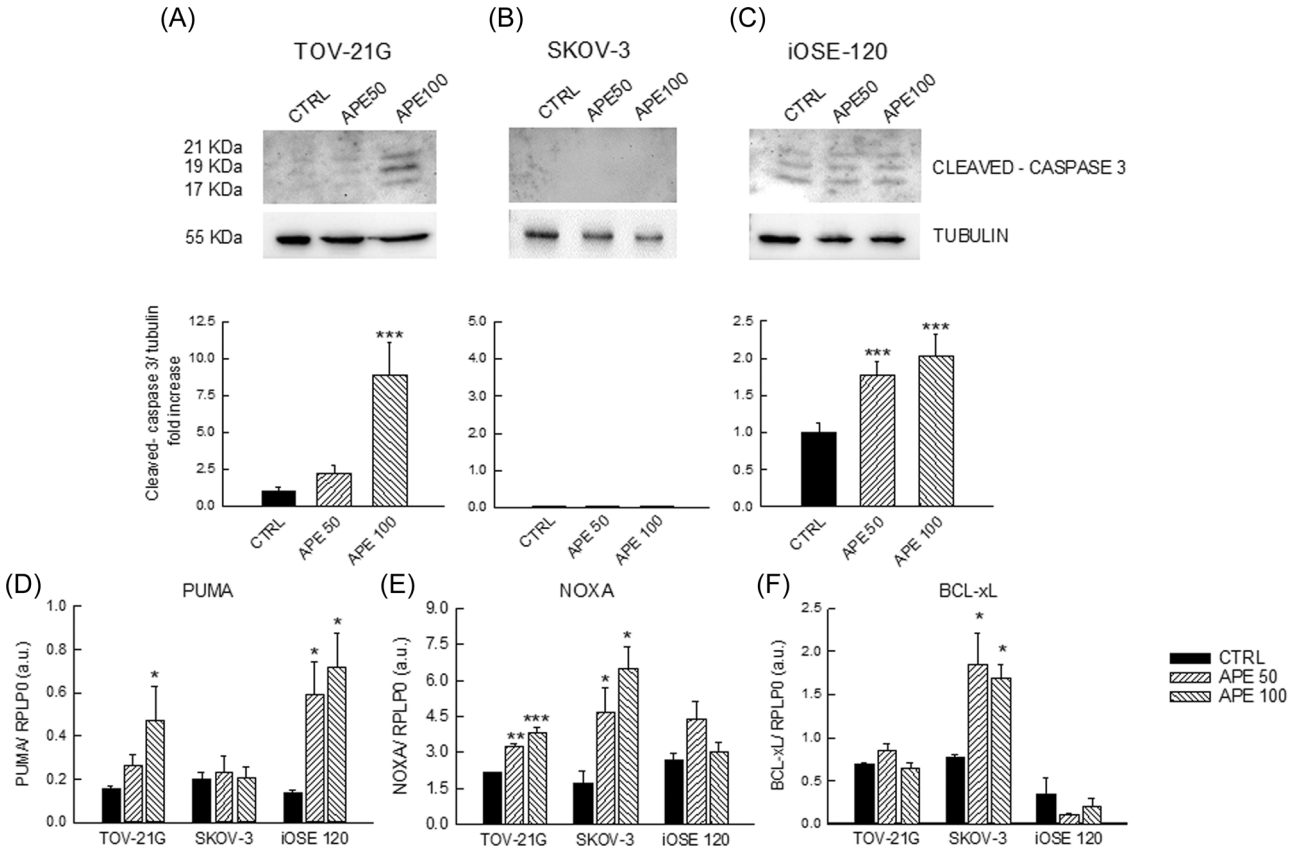

FIGURE 6 Western Blot analysis of Cleaved-caspase 3 expression in the different cell lines (A–C). In the figure is reported a representative blot. Densitometric absorbance values from three separate experiments were averaged (±SEM) and are expressed as fold increase respect to the respective control set equal to 1. Tubulin was used as internal control. ***$p < 0.001$ versus control (CTRL). (D–F) Levels of expression of *PUMA, NOXA*, and *BCL-xL* genes analyzed by Real Time-PCR in the different cell lines. The levels of the transcripts were normalized with the housekeeping gene (RPLP0). Data are the mean ± SEM of three independent experiments performed in triplicate and are expressed as arbitrary units. *$p < 0.05$; **$p < 0.005$; ***$p < 0.001$ versus respective CTRL.

observed in other tumor types,[11,13] cells with mutated p53 fail to resolve the mitotic division or DNA damage and may undergo aberrant mitosis and mitotic catastrophe.[30,31] Mitotic catastrophe may cause cell death following abnormal mitosis in cells presenting defects in checkpoint functions.[32] This hypothesis was confirmed by a high number of aberrant mitosis in APE-treated SKOV-3 and their absence in TOV-21G and by the different profiles obtained by cytofluorimetric analyses with Annexin V-APC/PI.

Moreover, the expression levels of gene involved in cell death were differently modulated in the three cell lines. APE treatment induced *PUMA* (p53 upregulated modulator of apoptosis), and *NOXA* in both iOSE-120 and TOV-21G, while *NOXA* but not *PUMA* was induced in SKOV-3 cells, which do not express endogenous p53. Interestingly, in APE-treated cells, cleaved caspase-3 was readily induced in TOV-21G and iOSE-120 but not in SKOV cells, while induction of *BCL-xL* was observed in SKOV but not in TOV-21G and iOSE-120. These data are in line with published results showing that BCL-xL is already expressed in SKOV-3, and its expression increases upon stimulation with BPR0L075, a novel synthetic indole compound that inhibits tubulin polymerization.[33] Interestingly, in SKOV3, BPR0L075 induced an alternative, caspase-3 independent, cell death by mitotic catastrophe.[33] Caspase-3 is considered a key effector enzyme in inducing cell apoptosis. Bcl-xL is an inhibitor of the Bcl-2 family of apoptotic proteins and is associated with resistance to antitumoral agents in many tumor types.[34] In addition to its involvement in apoptosis, Bcl-xL overexpression increases the aggressiveness of cancer cells by positively regulating invasion and migration, promoting tumor angiogenesis, and maintaining cancer stem cell phenotype.[35] In the literature, a relation between caspase-3 and Bcl-xL activities has been described. It has been shown that Bcl-xL could block the activation of caspase-3,[36] while in polymorphonuclear neutrophils, caspase-3 may regulate Bcl-xL levels by direct proteolytic cleavage.[37] The induction of *BCL-xL* in

SKOV-3, but not in the other cell lines, may explain the different cell death responses upon APE treatment in the different cell lines. In fact, in hepatocellular carcinoma, it has been shown that even though *BCL-xL* overexpression effectively blocked doxorubicin-induced apoptosis, however, it did not prevent doxorubicin-induced cell death through mitotic catastrophe.[38]

In every ovulatory cycle, OSE cells are injured, and subsequently, through repair mechanisms, the cells undergo cyclical ovulatory ruptures and repair, leading to a predisposition to developing mutation and, later, malignancies.[4] OSE cells can be influenced by several factors and hormones present in their environment.[39,40] It has been demonstrated that gonadotropins (FSH and luteinizing hormone [LH]) may regulate OSE cells proliferation and selected ovarian tumors either directly through LH- and FSH-receptors or by stimulating the expression of growth factors such as KGF, HGF, and KL.[41–43] Moreover, granulosa cells produce ACh in response to FSH,[8] and the presence of mAChRs on OSE cells renders OSE cells responsive to ACh. Therefore, a correct balance of the different mAChR subtypes might be relevant for controlling OSE cell proliferation/death. The data showing the prevalence of M3 receptors in ovarian cancer[19] and the lower levels of M2 receptors, as demonstrated in the present work, further support the significant correlation between mAChR status and poor prognosis in patients with ovarian cancer.[18]

In conclusion, our results, according to the results obtained in other tumor types,[9,12,14,15,44] confirm the inhibitory role of M2 receptors on tumor cell proliferation and survival.

Although the nature of the effects produced by APE in ovarian cell lines requires further investigations, these results indicate that the M2 mAChR could represent a new promising tool to explore in ovarian cancer development and therapy. The identification of novel compounds able to overcome drug resistance that can be used as adjuvant along with chemotherapeutic drugs are needed to improve the survival of ovarian cancer patients. Moreover, the development of novel M2 subtypes specific agonists with higher affinity compared to APE that could be used at lower concentrations than APE may also represent new interesting therapeutic perspectives for the ovarian cancer treatment.[44,45]

AUTHOR CONTRIBUTIONS

Marilena Taggi, Andjela Kovacevic, Chiara Capponi, Marta Falcinelli, and Veronica Cacciamani performed experiments; Rita Canipari, Elena Vicini and Ada Maria Tata conceived, supervised the study, and analyzed data; Marilena Taggi and Rita Canipari wrote the manuscript; Elena Vicini and Ada Maria Tata revised the manuscript. All the authors read and approved the final version of the manuscript.

ACKNOWLEDGMENTS

We are grateful to Stefania Fera for excellent technical support. This study was supported by Ateneo Sapienza Funds to A. M. T., R. C. and Ministry of Research MIUR Grant PRIN 2017 2017TK7Z8L to Elena Vicini.

CONFLICT OF INTEREST

The authors declare no conflict of interest.

DATA AVAILABILITY STATEMENT

The data that support the findings of this study are available on request from the corresponding author.

ORCID

Elena Vicini https://orcid.org/0000-0003-0399-0145
Rita Canipari http://orcid.org/0000-0003-3481-6908
Ada Maria Tata https://orcid.org/0000-0003-4868-5435

REFERENCES

1. Cramer DW, Welch WR. Determinants of ovarian cancer risk. II. Inferences regarding pathogenesis. *J Natl Cancer Inst*. 1983;71(4):717-721.
2. Mertens-Walker I, Baxter RC, Marsh DJ. Gonadotropin signalling in epithelial ovarian cancer. *Cancer Lett*. 2012;324(2):152-159. doi:10.1016/j.canlet.2012.05.017
3. Halperin R, Pansky M, Vaknin Z, Zehavi S, Bukovsky I, Schneider D. Luteinizing hormone in peritoneal and ovarian cyst fluids: a predictor of ovarian carcinoma. *Eur J Obstet Gynecol Reprod Biol*. 2003;110(2):207-210. doi:10.1016/s0301-2115(03)00122-2
4. Fathalla MF. Incessant ovulation—a factor in ovarian neoplasia? *Lancet*. 1971;2(7716):163. doi:10.1016/s0140-6736(71)92335-x
5. Gubbay O, Guo W, Rae MT, Niven D, Langdon SP, Hillier SG. Inflammation-associated gene expression is altered between normal human ovarian surface epithelial cells and cell lines derived from ovarian adenocarcinomas. *Br J Cancer*. 2005;92(10):1927-1933. doi:10.1038/sj.bjc.6602568
6. Altinoz MA, Korkmaz R. NF-kappaB, macrophage migration inhibitory factor and cyclooxygenase-inhibitions as likely mechanisms behind the acetaminophen- and NSAID-prevention of the ovarian cancer. *Neoplasma*. 2004;51(4):239-247.
7. Fritz S, Wessler I, Breitling R, et al. Expression of muscarinic receptor types in the primate ovary and evidence for nonneuronal acetylcholine synthesis. *J Clin Endocrinol Metab*. 2001;86(1):349-354. doi:10.1210/jcem.86.1.7146
8. Mayerhofer A, Kunz L. A non-neuronal cholinergic system of the ovarian follicle. *Ann Anat*. 2005;187(5-6):521-528. doi:10.1016/j.aanat.2005.06.005
9. Espanol AJ, Salem A, Di Bari M, et al. The metronomic combination of paclitaxel with cholinergic agonists inhibits triple negative breast tumor progression. Participation of M2

receptor subtype. *PLoS One*. 2020;15(9):e0226450. doi:10.1371/journal.pone.0226450
10. Luciano AM, Tata AM. Functional Characterization of Cholinergic Receptors in Melanoma Cells. *Cancers (Basel)*. 2020;12(11):3141. doi:10.3390/cancers12113141
11. Lucianò AM, Perciballi E, Fiore M, Del Bufalo D, Tata AM. The combination of the M2 muscarinic receptor agonist and chemotherapy affects drug resistance in neuroblastoma cells. *Int J Mol Sci*. 2020;21(22):8433. doi:10.3390/ijms21228433
12. Alessandrini F, Cristofaro I, Di Bari M, Zasso J, Conti L, Tata AM. The activation of M2 muscarinic receptor inhibits cell growth and survival in human glioblastoma cancer stem cells. *Int Immunopharmacol*. 2015;29(1):105-109. doi:10.1016/j.intimp.2015.05.032
13. Cristofaro I, Alessandrini F, Spinello Z, et al. Cross interaction between M2 muscarinic receptor and Notch1/EGFR pathway in human glioblastoma cancer stem cells: effects on cell cycle progression and survival. *Cells*. 2020;9(3):657. doi:10.3390/cells9030657
14. Di Bari M, Tombolillo V, Conte C, et al. Cytotoxic and genotoxic effects mediated by M2 muscarinic receptor activation in human glioblastoma cells. *Neurochem Int*. 2015;90:261-270. doi:10.1016/j.neuint.2015.09.008
15. Ferretti M, Fabbiano C, Di Bari M, et al. M2 receptor activation inhibits cell cycle progression and survival in human glioblastoma cells. *J Cell Mol Med*. 2013;17(4):552-566. doi:10.1111/jcmm.12038
16. Kistemaker LE, Oenema TA, Meurs H, Gosens R. Regulation of airway inflammation and remodeling by muscarinic receptors: perspectives on anticholinergic therapy in asthma and COPD. *Life Sci*. 2012;91(21-22):1126-1133. doi:10.1016/j.lfs.2012.02.021
17. Mayerhofer A, Fritz S. Ovarian acetylcholine and muscarinic receptors: hints of a novel intrinsic ovarian regulatory system. *Microsc Res Tech*. 2002;59(6):503-508. doi:10.1002/jemt.10228
18. Oppitz M, Mobus V, Brock S, Drews U. Muscarinic receptors in cell lines from ovarian carcinoma: negative correlation with survival of patients. *Gynecol Oncol*. 2002;85(1):159-164. doi:10.1006/gyno.2002.6597
19. Batra S, Popper LD, Iosif CS. Characterisation of muscarinic cholinergic receptors in human ovaries, ovarian tumours and tumour cell lines. *Eur J Cancer*. 1993;29A(9):1302-1306. doi:10.1016/0959-8049(93)90078-t
20. Piovesana R, Melfi S, Fiore M, Magnaghi V, Tata AM. M2 muscarinic receptor activation inhibits cell proliferation and migration of rat adipose-mesenchymal stem cells. *J Cell Physiol*. 2018;233(7):5348-5360. doi:10.1002/jcp.26350
21. Loreti S, Ricordy R, De Stefano ME, Augusti-Tocco G, Tata AM. Acetylcholine inhibits cell cycle progression in rat Schwann cells by activation of the M2 receptor subtype. *Neuron Glia Biol*. 2007;3(4):269-279. doi:10.1017/S1740925X08000045
22. Laemmli UK. Cleavage of structural proteins during the assembly of the head of bacteriophage T4. *Nature*. 1970;227(5259):680-685. doi:10.1038/227680a0
23. Lee LH, Yang H, Bigras G. Current breast cancer proliferative markers correlate variably based on decoupled duration of cell cycle phases. *Sci Rep*. 2014;4:5122. doi:10.1038/srep05122
24. Spindel ER. Muscarinic receptor agonists and antagonists: effects on cancer. *Handb Exp Pharmacol*. 2012;208:451-468. doi:10.1007/978-3-642-23274-9_19
25. Ferretti M, Fabbiano C, Di Bari M, Ponti D, Calogero A, Tata AM. M2 muscarinic receptors inhibit cell proliferation in human glioblastoma cell lines. *Life Sci*. 2012;91(21-22):1134-1137. doi:10.1016/j.lfs.2012.04.033
26. Pacini L, De Falco E, Di Bari M, et al. M2muscarinic receptors inhibit cell proliferation and migration in urothelial bladder cancer cells. *Cancer Biol Ther*. 2014;15(11):1489-1498. doi:10.4161/15384047.2014.955740
27. Di Bari M, Tombolillo V, Alessandrini F, et al. M2 muscarinic receptor activation impairs mitotic progression and bipolar mitotic spindle formation in human glioblastoma cell lines. *Cells*. 2021;10(7):1727. doi:10.3390/cells10071727
28. Yaginuma Y, Westphal H. Abnormal structure and expression of the p53 gene in human ovarian carcinoma cell lines. *Cancer Res*. 1992;52(15):4196-4199.
29. Castedo M, Perfettini JL, Roumier T, Andreau K, Medema R, Kroemer G. Cell death by mitotic catastrophe: a molecular definition. *Oncogene*. 2004;23(16):2825-2837. doi:10.1038/sj.onc.1207528
30. Bertheau P, Lehmann-Che J, Varna M, et al. p53 in breast cancer subtypes and new insights into response to chemotherapy. *Breast*. 2013;22(suppl 2):S27-S29. doi:10.1016/j.breast.2013.07.005
31. Vakifahmetoglu H, Olsson M, Tamm C, Heidari N, Orrenius S, Zhivotovsky B. DNA damage induces two distinct modes of cell death in ovarian carcinomas. *Cell Death Differ*. 2008;15(3):555-566. doi:10.1038/sj.cdd.4402286
32. Roninson IB, Broude EV, Chang BD. If not apoptosis, then what? Treatment-induced senescence and mitotic catastrophe in tumor cells. *Drug Resist Updat*. 2001;4(5):303-313. doi:10.1054/drup.2001.0213
33. Wang X, Wu E, Wu J, Wang TL, Hsieh HP, Liu X. An antimitotic and antivascular agent BPR0L075 overcomes multidrug resistance and induces mitotic catastrophe in paclitaxel-resistant ovarian cancer cells. *PLoS One*. 2013;8(6):e65686. doi:10.1371/journal.pone.0065686
34. Frenzel A, Grespi F, Chmelewskij W, Villunger A. Bcl2 family proteins in carcinogenesis and the treatment of cancer. *Apoptosis*. 2009;14(4):584-596. doi:10.1007/s10495-008-0300-z
35. Trisciuoglio D, Tupone MG, Desideri M, et al. BCL-XL overexpression promotes tumor progression-associated properties. *Cell Death Dis*. 2017;8(12):3216. doi:10.1038/s41419-017-0055-y
36. Salvesen GS, Dixit VM. Caspases: intracellular signaling by proteolysis. *Cell*. 1997;91(4):443-446. doi:10.1016/s0092-8674(00)80430-4
37. Weinmann P, Gaehtgens P, Walzog B. Bcl-Xl- and Bax-alpha-mediated regulation of apoptosis of human neutrophils via caspase-3. *Blood*. 1999;93(9):3106-3115.
38. Park SS, Kim MA, Eom YW, Choi KS. Bcl-xL blocks high dose doxorubicin-induced apoptosis but not low dose doxorubicin-induced cell death through mitotic catastrophe. *Biochem Biophys Res Commun*. 2007;363(4):1044-1049. doi:10.1016/j.bbrc.2007.09.037
39. Leung PC, Choi JH. Endocrine signaling in ovarian surface epithelium and cancer. *Hum Reprod Update*. 2007;13(2):143-162. doi:10.1093/humupd/dml002
40. Riman T, Persson I, Nilsson S. Hormonal aspects of epithelial ovarian cancer: review of epidemiological evidence. *Clin*

Endocrinol (Oxf). 1998;49(6):695-707. doi:10.1046/j.1365-2265.1998.00577.x

41. Parrott JA, Kim G, Mosher R, Skinner MK. Expression and action of keratinocyte growth factor (KGF) in normal ovarian surface epithelium and ovarian cancer. *Mol Cell Endocrinol*. 2000;167(1-2):77-87. doi:10.1016/s0303-7207(00)00284-7
42. Parrott JA, Kim G, Skinner MK. Expression and action of kit ligand/stem cell factor in normal human and bovine ovarian surface epithelium and ovarian cancer. *Biol Reprod*. 2000;62(6):1600-1609. doi:10.1095/biolreprod62.6.1600
43. Parrott JA, Skinner MK. Expression and action of hepatocyte growth factor in human and bovine normal ovarian surface epithelium and ovarian cancer. *Biol Reprod*. 2000;62(3):491-500. doi:10.1095/biolreprod62.3.491
44. Guerriero C, Matera C, Del Bufalo D, et al. The combined treatment with chemotherapeutic agents and the dualsteric muscarinic agonist Iper-8-naphthalimide affects drug resistance in glioblastoma stem cells. *Cells*. 2021;10(8):1877. doi:10.3390/cells10081877
45. Cristofaro I, Spinello Z, Matera C, et al. Activation of M2 muscarinic acetylcholine receptors by a hybrid agonist enhances cytotoxic effects in GB7 glioblastoma cancer stem cells. *Neurochem Int*. 2018;118:52-60. doi:10.1016/j.neuint.2018.04.010

SUPPORTING INFORMATION

Additional supporting information can be found online in the Supporting Information section at the end of this article.

How to cite this article: Taggi M, Kovacevic A, Capponi C, et al. The activation of M2 muscarinic receptor inhibits cell growth and survival in human epithelial ovarian carcinoma. *J Cell Biochem*. 2022;1-14. doi:10.1002/jcb.30303